








Article

Modeling and Optimization of Biochar Based Adsorbent Derived from Kenaf Using Response Surface Methodology on Adsorption of Cd²⁺

Anwar Ameen Hezam Saeed ^{1,2}, Noorfidza Yub Harun ^{1,2,*}, Suriati Sufian ¹, Muhammad Roil Bilad ³, Baiq Asma Nufida ³, Noor Maizura Ismail ^{4,*}, Zaki Yamani Zakaria ⁵, Ahmad Hussaini Jagaba ⁶, Aiban Abdulhakim Saeed Ghaleb ⁵ and Baker Nasser Saleh Al-Dhawi ⁶

- ¹ Department of Chemical Engineering, Universiti Teknologi PETRONAS, Bandar Seri Iskandar 32610, Perak Darul Ridzuan, Malaysia; anwar_17006829@utp.edu.my (A.A.H.S.); suriati@utp.edu.my (S.S.)
- ² Centre of Urban Resource Sustainability, Universiti Teknologi PETRONAS, Bandar Seri Iskandar 32610, Perak Darul Ridzuan, Malaysia
- ³ Faculty of Applied Science and Engineering, Universitas Pendidikan Mandalika (UNDIKMA), Jl. Pemuda No. 59A, Mataram 83126, Indonesia; muhammadroilbilad@ikipmataram.ac.id (M.R.B.); baiqasmanufida@ikipmataram.ac.id (B.A.N.)
- ⁴ Faculty of Engineering, Universiti Malaysia Sabah, Jln UMS, Kota Kinabalu 88400, Sabah, Malaysia
- ⁵ School of Chemical & Energy Engineering, Universiti Teknologi Malaysia, Skudai 81310, Johor, Malaysia; zakiyamani@utm.my (Z.Y.Z.); aiban_17004546@utp.edu.my (A.A.S.G.)
- ⁶ Department of Civil and Environmental Engineering, Universiti Teknologi PETRONAS, Bandar Seri Iskandar 32610, Perak Darul Ridzuan, Malaysia; ahmad_19001511@utp.edu.my (A.H.J.); baker_18002007@utp.edu.my (B.N.S.A.-D.)
- * Correspondence: noorfidza.yub@utp.edu.my (N.Y.H.); maizura@ums.edu.my (N.M.I.)



Citation: Saeed, A.A.H.; Harun, N.Y.; Sufian, S.; Bilad, M.R.; Nufida, B.A.; Ismail, N.M.; Zakaria, Z.Y.; Jagaba, A.H.; Ghaleb, A.A.S.; Al-Dhawi, B.N.S. Modeling and Optimization of Biochar Based Adsorbent Derived from Kenaf Using Response Surface Methodology on Adsorption of Cd²⁺. *Water* **2021**, *13*, 999. <https://doi.org/10.3390/w13070999>

Academic Editors: Mika Sillanpää and Peyman Gholami

Received: 7 March 2021

Accepted: 29 March 2021

Published: 5 April 2021

Publisher's Note: MDPI stays neutral with regard to jurisdictional claims in published maps and institutional affiliations.



Copyright: © 2021 by the authors. Licensee MDPI, Basel, Switzerland. This article is an open access article distributed under the terms and conditions of the Creative Commons Attribution (CC BY) license (<https://creativecommons.org/licenses/by/4.0/>).

Abstract: Cadmium is one of the most hazardous metals in the environment, even when present at very low concentrations. This study reports the systematic development of Kenaf fiber biochar as an adsorbent for the removal of cadmium (Cd) (II) ions from water. The adsorbent development was aided by an optimization tool. Activated biochar was prepared using the physicochemical activation method, consisting of pre-impregnation with NaOH and nitrogen (N₂) pyrolysis. The influence of the preparation parameters—namely, chemical impregnation (NaOH: KF), pyrolysis temperature, and pyrolysis time on biochar yield, removal rate, and the adsorption capacity of Cd (II) ions—was investigated. From the experimental data, some quadratic correlation models were developed according to the central composite design. All models demonstrated a good fit with the experimental data. The experimental results revealed that the pyrolysis temperature and heating time were the main factors that affected the yield of biochar and had a positive effect on the Cd (II) ions' removal rate and adsorption capacity. The impregnation ratio also showed a positive effect on the specific surface area of the biochar, removal rate, and adsorption capacity of cadmium, with a negligible effect on the biochar yield. The optimal biochar-based adsorbent was obtained under the following conditions: 550 °C of pyrolysis temperature, 180 min of heating time, and a 1:1 NaOH impregnation ratio. The optimum adsorbent showed 28.60% biochar yield, 69.82% Cd (II) ions removal, 23.48 mg/g of adsorption capacity, and 160.44 m²/g of biochar-specific area.

Keywords: biochar; cadmium; optimization; adsorption; kenaf fiber; CCD-RSM

1. Introduction

The rapid industrial developments such as metal plating facilities, textile dyeing, leather tanning, paint and pigment manufacturing, fertilizers, tanneries, batteries, paper, and pesticides, as well as metal finishing industries, result in heavy metal accumulation in the environment [1,2]. Heavy metals are elements with an atomic weight of 63.5 to

200.6 g/mol, with a specific gravity of greater than 5 [3]. Heavy metals can be essential or deadly based on their concentration and toxicity level [4]. Essential heavy metals include zinc, copper, iron, chromium, cobalt, and selenium. They are required for regular body functions, as long as they are present at the permissible limit [5,6]. On the other hand, nonessential heavy metals, such as cadmium, mercury, lead, and arsenic, are extremely toxic, even at low concentrations [7]. The toxic heavy metals can affect the human body and may cause acute or chronic effects, be carcinogenic, or may lead to digestive and nervous system diseases [8,9].

Cadmium is one of the most hazardous metals. Yet, it is used in many industries, including paint, batteries, and dyes [10]. Cadmium is used in a form of cadmium nitrate and cadmium sulfate and tends to leach into the environment [11]. Due to cadmium's persistent and toxicity characteristics, it is listed in the US Environmental Protection Agency under Priority Control Pollutant List [12]. The United States Environmental Protection Agency has also set the permissible concentration of cadmium in drinking water at 5 ppb, slightly higher than the World Health Organization of 3 ppb [13]. Cadmium contamination causes severe health risks upon exposure. Compounds of cadmium are very toxic; absorption at a high level by the body can lead to various disorders, such as blood pressure and heart diseases, and can even cause death [14]. Cadmium is dangerous not only because of its high toxicity but, also, because of the proliferation of its compounds in several industries, such as batteries, alloys, coatings (electroplating), solar cells, plastic stabilizers, and pigments [15]. Cadmium is derived from zinc byproducts and extracted from recycled batteries with nickel–cadmium [16].

The treatments for removing heavy metals are many. They include ion exchanges, chemical precipitation, filtration, and adsorption. Recently, adsorption is considered an attractive method due to its simplicity, cost-effectiveness, and the possibility of using it on a larger scale [17,18]. Many adsorbent materials have been applied in industries—namely, activated carbon, activated alumina, silica gel, molecular sieve carbon, molecular sieve zeolites, and polymeric adsorbents [19–21].

Several adsorbents, like graphene oxide [22], the metal–organic framework [23], zeolites [24], activated biochar [25], carbon nanotubes [26], activated carbon [27], and many others, have recently been developed for the removal of heavy metals from aqueous solutions. However, when compared to agricultural-based adsorbents, they are often more expensive [28].

Kenaf or *Hibiscus cannabinus* is a plant of the Malvaceae family that grows in tropical and subtropical areas [29]. It typically consists of cellulose (33–42%), hemicellulose (21.50%), lignin (15–19%), and mineral ash (2.5–4%) [30]. It has been widely explored as a feedstock for adsorbents. Recently, numerous attempts have been reported on the use of biochar extracted from agricultural waste for the removal of heavy metals from water [31,32].

Biochar has the same properties as activated carbon, which makes it promising as an adsorbent. The chemical and physical characteristics of biochar differ based on the quality of the raw materials, method, temperature, and time of pyrolysis, as well as chemical modification of the biochar by exposure to acids or alkalis [33,34]. Many variables affect the composition of biochar. Biochar is typically rich in functional groups such as hydroxyl, carboxyl, carbonyl, and methylene on the surfaces of the pore system [35]. Biochar has a large surface area and strong adsorption efficiency that makes it attractive for the removal of heavy metals from wastewater [36].

This study investigates and optimizes the adsorption of cadmium (Cd) (II) from a synthetic aqueous solution by kenaf-activated biochar. Response surface methodology (RSM) was applied to help with the optimization of the preparation parameters. The application of RSM allowed a minimal number of tests, and the software is incorporated with mathematical and statistical tools and, as such, can be used to analyze interactions between parameters [37–39]. Some of the previous studies used RSM in the preparation of activated carbons using precursors such as olive-waste cakes [40], rice husks [41], and Luscar char [42]. Monik Kasman [43] applied RSM to study cadmium removal by using

raw rice husks and found that raw rice husks poorly adsorbed cadmium with 70% removal, suggesting the need for adsorbent improvement. Taimur Khan [44] found that rice husk carbon was a sufficient adsorbent for lead removal after optimization with an artificial neural network during the adsorbent development. Raphael et al. also reported the adsorption of Cadmium from water using Raffia Palm seed (*Raphia hookeri*)-activated carbon as an adsorbent [45].

To date, there has been no research on the preparation of biochar from the Kenaf fiber using the RSM method by a physicochemical activation method, including NaOH impregnation and N₂ Pyrolysis. This study implemented a central composite design to evaluate the effect of the input parameters during the preparation of the biochar. The input parameters included the pyrolysis temperature, pyrolysis time, and chemical impregnation (NaOH/KF) on the four response parameters of the adsorption capacity, removal efficiency, specific surface area, and biochar yield.

2. Materials and Methods

2.1. Collection, Purification, and Preparation of Materials

The Kenaf fiber was obtained from the Kenaf plantation in Pahang, Malaysia. It was washed continuously with distilled water 3–5 times to remove the impurities and dust from its surface, followed by drying in an oven (Thermo Scientific Vac Oven 65.1 L 120,401 Millcreek Road, Marietta, OH 45750, United States) at 105 °C for 24 h. The dried sample was ground by using a mechanical shredder machine (Granulator WSGP-230) and sieved using a vibratory sieve shaker to the desired mesh size of 1 to 2 mm. It was then placed in an airtight container at room temperature before using it. The other chemicals, such as sodium hydroxide, hydrochloric acid, cadmium nitrate trihydrate, ferrous and ferric chloride, and ethanol, were bought from Sigma-Aldrich. The chemicals were used as received without any treatment.

2.2. Biochar Based Adsorbent Preparation (Design of Experiments)

The pyrolysis was performed by placing the samples in an Alumina Tube Furnace under different input parameters, as presented in Table 1. Purified nitrogen (99.995%) with a flow rate of 100 cm³/min was used, under a heating rate of 10 °C/min during the pyrolysis process.

Table 1. Independent variables and their coded and actual levels for the central composite design for the preparation of biochar.

Parameters	Units	Code	Ranges and Coded Levels				
			− α	−1	0	+1	+ α
Pyrolysis Temperature	°C	X ₁	197	300	450	600	702
Reaction time	Minutes	X ₂	19	60	120	180	220
Impregnation ratio	w/w	X ₃	0.32	1	2	3	3.68

Determination of the value of parameters in Table 1 was done using the design of the experiment via RSM. RSM is usually carried out to widen the screening mathematical and statistical methods for analyzing and improving products, which are followed up by experimental quantitative data to determine the regression models and optimal operating conditions. A highly accurate second-order quadratic model was composed by CCD with the minimum possible number of experiments [46].

The value range of the pyrolysis temperature for kenaf was 300–600 °C. The range was selected based on values recommended from previous studies [34,47,48], which stated that the kenaf mass loss was attributed to three main stages: drying and evaporation of light particles (stage I), volatilization of hemicellulose and cellulose (stage II), and decomposition of lignin (stage III). Stage I happened at temperatures below 150 °C, stage II started degassing from 150 to 375 °C, and finally, stage III at temperatures above 400 °C. For that reason, the recommended range of pyrolysis temperature was 300–600 °C, which

helped in converting the lignin into biochar and kept biochar stable. The effect of residence time is often dominated by the pyrolysis temperature. Therefore, it is sometimes hard to give a straightforward value for the role of residence time in biochar stability. Therefore, a big range value was assigned to the reaction time parameter [49,50]. The selection of the heating rate was at 10 °C/min, which was considered low but favorable for producing biochar derived from agricultural feedstocks [50,51]. Furthermore, a lower heating rate (10 °C/min) could facilitate the aromatic structure formation in biochar. Moreover, a low heating rate favored the retention of structural complexity, while the loss of structural complexity would happen at a high heating rate due to the local melting of cell structures, phase transformations, and swelling [52].

The obtained biochar was activated by the physicochemical method by changing the preparation parameters. The parameters were pyrolysis temperature (X_1), pyrolysis time (X_2), and the impregnation ratio (X_3) of NaOH:KF. Sodium hydroxide (NaOH) was used for the chemical activation process because of its good efficiency in enhancing the surface properties of activated biochar during the pyrolysis process [53]. These three parameters were found to be the most important factors affecting the characteristics of biochar-based adsorbents [54]. Eight factor points and six axial points and center points were scheduled for the central composite design. There were five levels of selected factors ($-\alpha$, -1 , 0 , 1 , and $+\alpha$), resulting in the number of experiments of 20. Table 1 indicates the lower and higher limits of every factor. The data were processed using the analysis of variance (ANOVA) and visualized using surface contour plots.

The central points were used to determine the experiment errors and data repeatability. The independent parameters were labeled at intervals of $(-1, 1)$, with low and high values assigned, respectively, to -1 and $+1$. The axial points were positioned at $(\pm\alpha, 0, 0)$, $(0, \pm\alpha, 0)$, and $(0, 0, \pm\alpha)$, where α is the distance from the axial points to the central point, making the design, which is fixed, at 1.682 mm.

For the adsorption study, 1000 mg/L Cd (II) stock solution was prepared by dissolving cadmium nitrate trihydrate. The stock solution was diluted to 25 mg/L of Cd^{2+} for batch studies. The solution was treated with a fixed variable to obtain the best pyrolysis process parameters for cadmium removal. The fixed parameters were the dose of the adsorbent, the pH of the solution, the stirring speed, and adsorption time. The pH of the solution was adjusted to 6.0, because a previous study [55] proved that the Cd^{2+} ions could be adsorbed at that pH value. The rotation speed and time were fixed at 200 rpm for 1 h [56]. The sample before and after adsorption was collected and analyzed for the cadmium concentration by flame atomic absorption spectrometry. The difference between the initial and final (or equilibrium) Cd^{2+} concentrations determined the amount of Cd^{2+} absorbed by the kenaf-based biochar. The yield, removal efficiency, and adsorption capacity of kenaf-based biochar were calculated according to Equations (1)–(3).

$$\text{Biochar Yield\%} = \frac{W_b}{W_r} \times 100 \quad (1)$$

$$\text{Removal Efficiency \%} = \frac{C_i - C_e}{C_i} \times 100 \quad (2)$$

$$q_e = \frac{(C_i - C_e) \times (V)}{m} \quad (3)$$

where W_b and W_r are the weight of biochar and the weight of raw rice husks. C_i and C_e are the initial concentration and final concentration (mg/L), q_e (mg/g) is the adsorption capacity of biochar, m is the dry mass of biochar (g), and V is for the volume of the solution (L).

3. Results and Discussion

3.1. Effect of the Heating Temperature on Kenaf Biochar Yield and Cadmium Removal

Figure 1 shows the effect of the pyrolysis temperature on the biochar production yield. The heating temperature is one of the most important factors affecting the biochar properties. The biochar yield was achieved at low temperatures and vice versa. Figure 1 also shows a steep decline in the biochar yield at a higher temperature, in which the biochar percentage dropped from 45% (at 702 °C) to 25% (at 197 °C). The findings are strongly supported by the literature, as a more solid product (biochar) is produced by pyrolysis at a low heating temperature. Nizamuddin et al. found a similar result and attributed the trend to the conversion of solid carbon into a gaseous form [57]. Another plausible explanation is that the cellulose and hemicellulose biomass decompose at higher temperatures [58]. A similar trend was also reported by Delik Angir [59] on the impact of different pyrolysis temperatures (ranging from 350 °C to 650 °C) and different heating rates (10 °C/min, 30 °C/min, and 50 °C/min) on the biochar yield from the slow pyrolysis of safflower seed press cake. They attributed the low yield at a high temperature to a greater primary decomposition or through the secondary decomposition of char residues. In this study, the heating rate was kept at 10 °C/min to get the high yield [60].

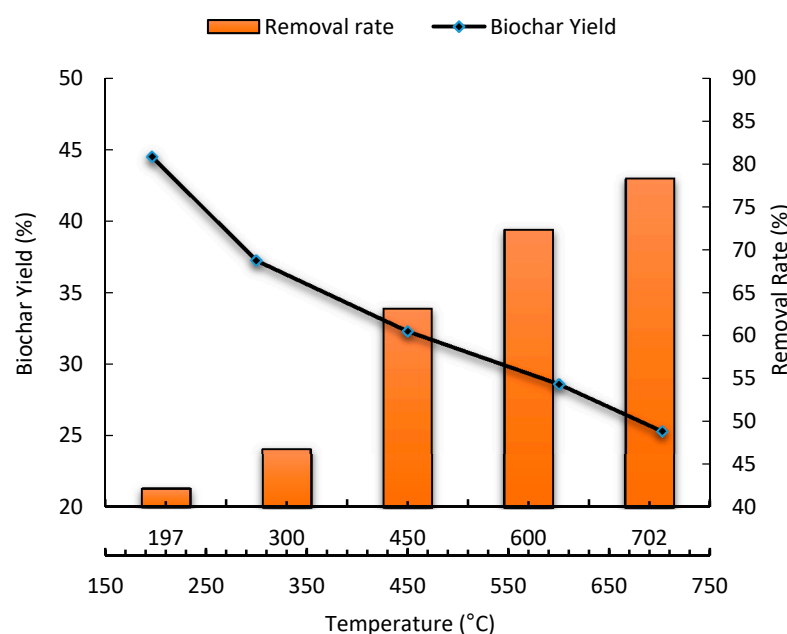


Figure 1. Temperature effect on the yield of Kenaf-based biochar and removal rate of cadmium.

Figure 1 also shows the effect of the heating temperature of the biochar-based adsorbent on the removal rate of cadmium. The removal rate of cadmium increases for the biochar produced at high temperatures. To justify the findings, Figure 2 was composed to show the proximate and ultimate analysis that tells how the O/C and H/C ratios affect the biochar properties. The O/C ratio indicates the polarity and abundance of the polar oxygen-containing surface functional groups in biochar. A higher O/C ratio indicates more polar functional groups [61], which actively take part in the adsorption of Cadmium. On the other hand, the H/C ratio indicates an aroma and stability of the biochar [62].

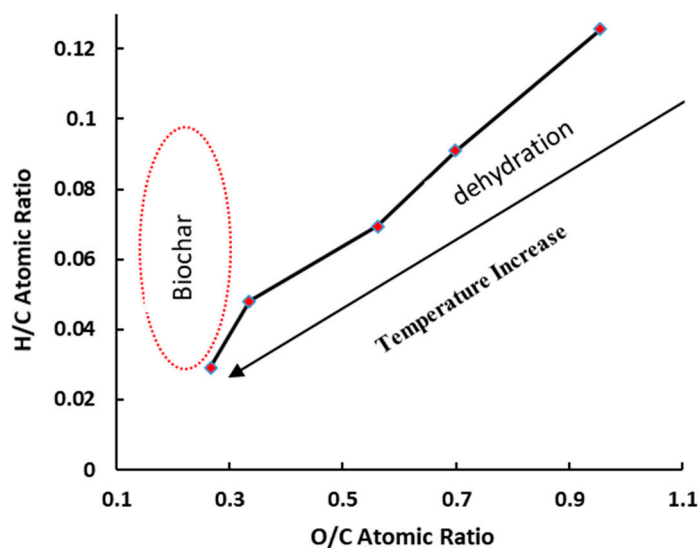


Figure 2. The Van Krevelen diagram comparing the O/C and H/C ratios of the prepared biochar.

3.2. Effect of the Heating Time on Biochar Yield and Cadmium Removal Rate

Figure 3 shows that the biochar yield is a function of the heating time. The yield decreases from 44% (20-min heating time) to 29% (220 min heating time). This finding is in line with the study reported by Tangjuank et al., in which the yield of biochar decreased from 82% to 64% when the activation time was increased from 20 to 150 min [63]. The trend can be ascribed by further decomposition at a prolonged heat exposure that led to the removal of volatile organic compounds, thereby reducing the biochar’s quantity [34].

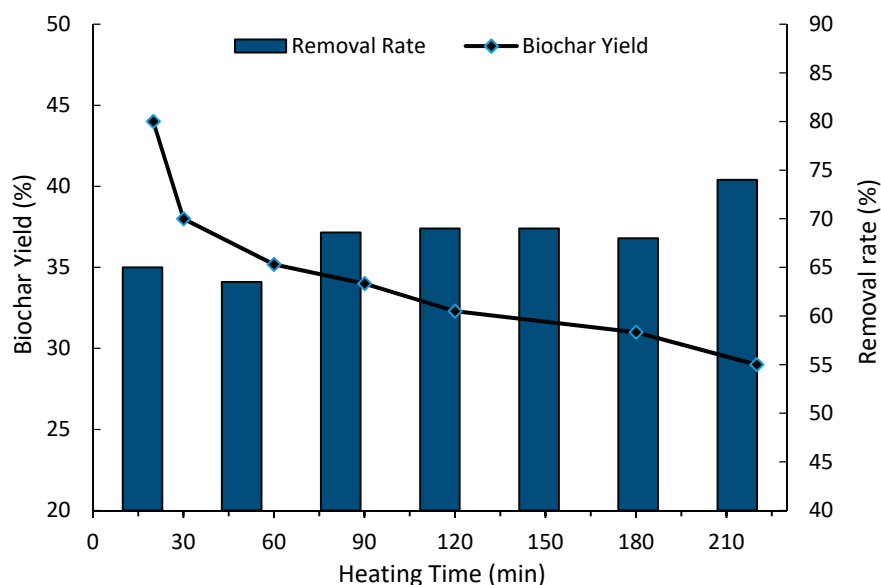


Figure 3. Effect of heating time on the biochar yield and removal rate of cadmium.

A long heating time enhanced the cadmium removal that increased from 68% to 74% with a longer heat time, from 180 to 220 min (Figure 3). This result is similar to the other study in which the removal rate and adsorption capacity of cadmium by biochar derived from *Eichhornia crassipes* increased from 96% to 99% and 9.63 mg/g to 9.90 mg/g with the increase in the heating time from one to two hours [64]. Due to the compensating effect of the yield and efficiency, it is important to perform parameter optimization to balance the removal efficiency and the biochar yield, as conducted via the RSM in this study.

3.3. Effect of the Impregnation Ratio on Biochar Yield and Cadmium Removal

Figure 4 displays the yield of impregnated biochar at different NaOH impregnation ratios. The yield of biochar was computed by dividing the final resultant biochar by the initial mass of impregnated raw material (Kenaf fiber). It shows that the impregnation ratio slightly affects the biochar yield of biochar because of the solubilization of NaOH in water during impregnation and due to the evaporation of water during biomass decomposition. A prominent effect of impregnation on cadmium removal is shown in Figure 4. Modification via surface oxidation has been shown to be effective in biochar development for heavy metal adsorption. It might increase some functional groups of biochar, such as carboxyl, phenol-based, quinonoid, lactone, and fluorescein [65]. Figure 4 also shows a maximum point of cadmium removal, suggesting the importance of synthesis method optimization. NaOH seems to positively affect cadmium removal, as also reported elsewhere [66].

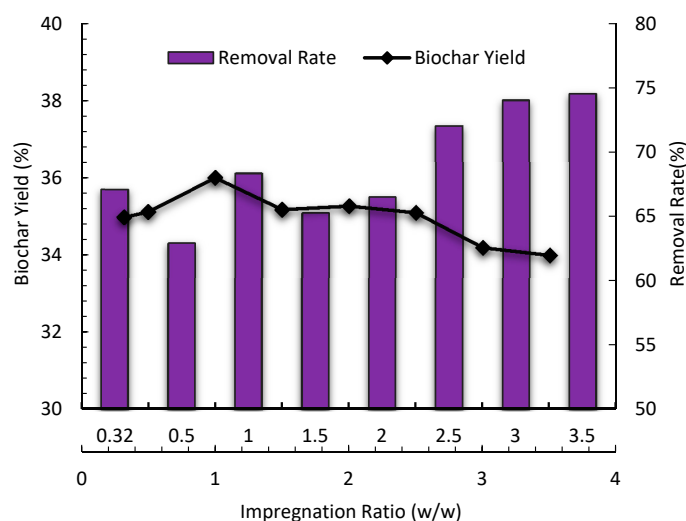


Figure 4. The effect of the impregnation ratio on the yield of biochar and removal rate of cadmium.

3.4. Effect of the Heating Temperature on Surface Area and Adsorption Capacity

Figure 5 shows that the surface area of the kenaf biochar increased with the increasing heating temperature. The attained biochar surface areas were 21 m²/g (at temperatures of 300–450 °C), 30 m²/g (450–600 °C), and 22 m²/g (600–700 °C). The increasing trend of the biochar surface area can be attributed to a large number of volatile compounds released during the carbonization process. When kenaf fiber is carbonized at low temperatures, the residue can block the pores due to incomplete carbonization [67].

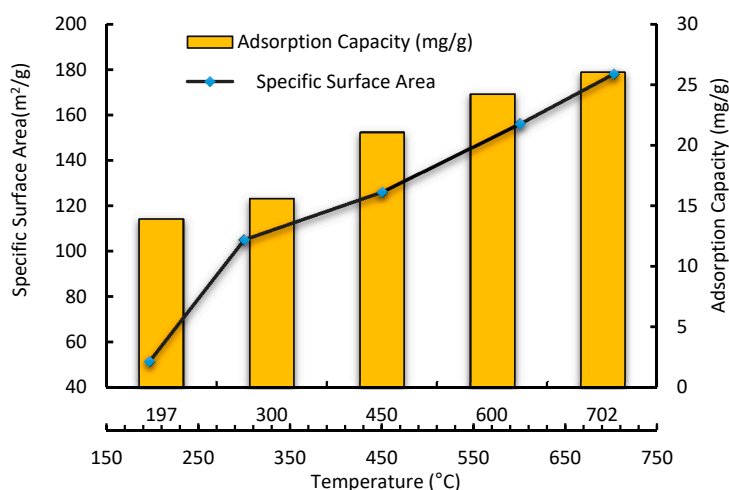


Figure 5. Effect on the biochar surface area and adsorption capacity.

Figure 5 also shows the effects of heating temperature on the adsorption capacity of kenaf biochar. When the heating temperature increased from 197 to 300 °C, there was a small increment of the adsorption capacity (from 13.9 mg/g to 15.58 mg/g). A jump in the adsorption capacity was observed under the heating temperature range of 300–400 °C, reaching an adsorption capacity value of 26 mg/g at 700 °C.

3.5. Effect of Heating Time on Surface Area and Adsorption Capacity

Figure 6 shows that the heating time during pyrolysis only slightly affects the biochar surface area. Conversely, the heating time showed an important effect up to 120 min. The adsorption capacity of Cd^{+2} by Kenaf biochar increased from 17.21 mg/g to 21 mg/g under a longer heating time, from 90 to 120 min.

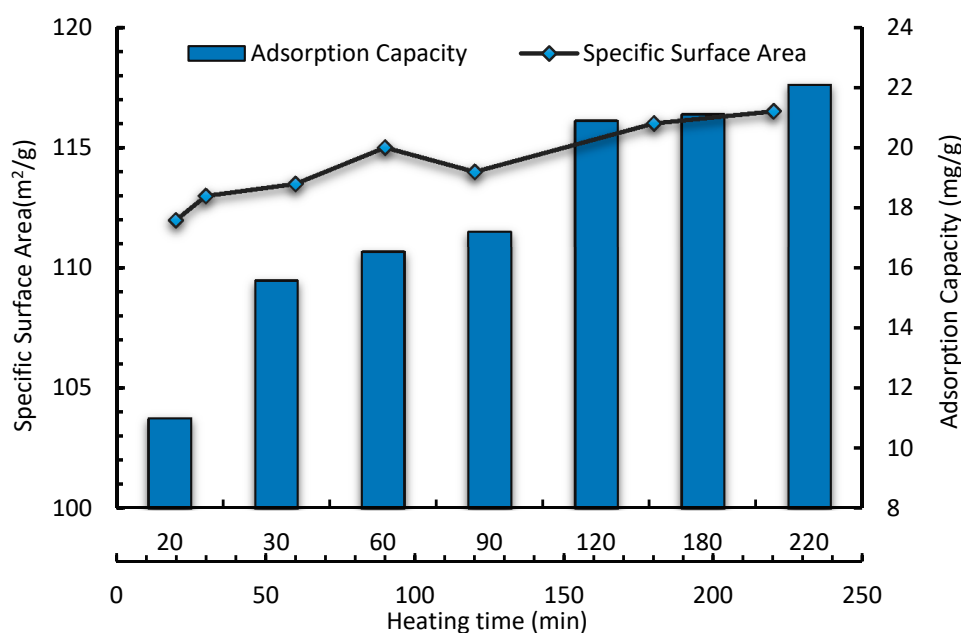


Figure 6. Effect of heating time on the biochar surface area and adsorption capacity.

3.6. Effect of Impregnation Ratio on Surface Area and Adsorption Capacity

Figure 7 shows that the best impregnation ratio of NaOH to Kenaf was 1:1, which resulted in a biochar surface area of 142 m²/g. Thanks to low alkali concentrations, the ester bond between lignin and sulfate could be broken via saponification, resulting in the degradation of lignin, which increased the selectivity [68]. This allowed the activator to access the raw material and increase the area of contact between the activator and the precursor of carbon [69]. Besides, during the alkaline leaching process, hemicellulose could be partly washed away. The leaching of hemicellulose may also lead to the formation of a porous structure and facilitate an intrusion of the activator into the substrate. The findings are in agreement with the one reported by Yang et al. [70], Kumar et al. [69], and Hara Mohan et al. [71] from other feedstocks. They found that the pretreatment of raw feedstocks with sodium hydroxide to produce activated biochar categorically improved the textural properties of biochar (such as the specific surface area and porosity).

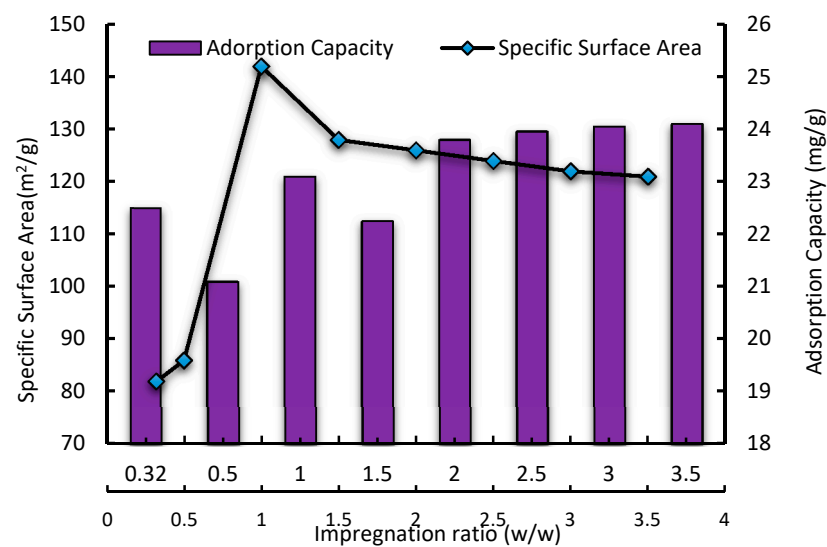


Figure 7. Impregnation ratio effect on the biochar surface area and adsorption capacity.

3.7. Statistical Analysis of Kenaf Biochar-Based Adsorbent Production

3.7.1. Development of the Regression Model

Table 2 displays the entire design matrix and the findings from the experiments to predict the optimal condition for the preparation and the interaction between the preparation conditions and the mathematical model shown in Equation (4). The responses were the biochar yield (Y_1), removal efficiency (Y_2), and adsorption capacity of cadmium (Y_3). Every response was designed to establish an empirical model that associated the response to modified biochar preparation variables with a polynomial second-degree equation, as in Equation (4) [72]:

$$Y = B_0 + B_1x_1 + B_2x_2 + B_3x_3 + B_{12}x_1x_2 + B_{13}x_1x_3 + B_{23}x_2x_3 + B_{11}x_1^2 + B_{22}x_2^2 + B_{33}x_3^2 \quad (4)$$

where Y is the predicted responses; B_0 the constant coefficient; B_1 , B_2 , and B_3 the linear coefficients, B_{12} , B_{13} , and B_{23} the binary interaction coefficients, B_{11} , B_{22} , and B_{33} the quadratic coefficients, and x_1 , x_2 , and x_3 are the coded values of the modified biochar preparation variables.

The input parameters and the response parameters are shown in Table 2. The biochar yield obtained ranged from 25% to 45%. The surface area of the biochar ranged from 51.5 m²/g to 178 m²/g. The cadmium removal rate and adsorption capacity ranged from 42.3% to 74.3% and from 14.1 mg/g to 26.10 mg/g, respectively. Based on the sequential square model sum, the models were chosen solely based on the better-order polynomials, where the additional parameters were scaled, and the models were no longer aliased. For the three response parameters: biochar yield, adsorption capacity, and cadmium removal, the quadratic model was recommended.

The final empirical models in terms of coded factors after an exception, the insignificant terms for Biochar yield (Y_1), cadmium removal (Y_2), adsorption capacity (Y_3), and specific surface area (Y_4) are shown in Equations (5)–(8):

$$Y_1 = +31.93 - 4.95X_1 - 1.715X_2 - 0.25X_3 + 0.92X_1X_2 + 0.56X_1X_3 - 0.44X_2X_3 + 0.96X_1^2 + 0.21X_2^2 + 0.15X_3^2 \quad (5)$$

$$Y_2 = +63.16 + 11.86X_1 + 0.86X_2 + 0.49X_3 - 0.98X_1X_2 - 0.48X_1X_3 - 0.43X_2X_3 - 1.40X_1^2 - 0.87X_2^2 - 0.18X_3^2 \quad (6)$$

$$Y_3 = +21.10 + 4.0X_1 + 0.31X_2 + 0.12X_3 - 0.24X_1X_2 - 0.075X_1X_3 - 0.23X_2X_3 + 0.51X_1^2 - 0.23X_2^2 - 0.0997X_3^2 \quad (7)$$

$$Y_4 = +121.78 + 34.30X_1 + 7.12X_2 - 1.00X_3 + 0.74X_1X_2 + 0.74X_2X_3 - 2.0X_2X_3 + 0.08X_1^2 + 1.73X_2^2 + 3.99X_3^2 \quad (8)$$

The interaction between the time (X_2) and impregnation ratios (X_3) was significant, with a negative impact on all four responses. The interaction with temperature (X_1) showed

a significant effect, with a positive sign ($B_{11} = 0.96$ for biochar yield, $B_{11} = 0.080$ for the specific surface area of biochar, and $B_{11} = 0.50$ for the adsorption capacity). The positive sign in front of the terms given in Equations (5)–(8) suggests a synergistic effect, while the negative signs indicate antagonistic impacts. The coefficient with one factor represents the influence of the particular factor, while the coefficient with the two factors and those with second-order terms represent the interaction between two factors and the quadratic effect, respectively.

Table 2. Experimental data obtained based on a central composite design.

Run	CCD Position	Biochar Preparation Variables			Responses			
		X_1 , Temperature (°C)	X_2 , Time (min)	X_3 , Impregnation Ratio (w/w)	Y_1 , Biochar Yield%	Y_2 , Cd (II) Removal (%)	Y_3 , Adsorption Capacity (mg/g)	Y_4 , SSA (m^2/g)
1	Factorial	300	180	1	36.1	49.5	16.5	109.4
2	Factorial	600	60	3	30.3	71.2	24.1	158.6
3	Axial	450	120	0.32	32.4	62.3	20.8	129.2
4	Axial	198	120	2	44.4	42.3	14.1	51.5
5	Axial	450	19	2	34.1	59.1	19.7	107.5
6	Factorial	300	60	3	40.5	48.3	16.1	94.5
7	Center	450	120	2	33.4	63.1	21.1	122.5
8	Factorial	600	60	1	29.9	74.3	24.8	153.5
9	Axial	450	220.10	2	31.3	66.2	22.1	133.4
10	Center	450	120	2	32.3	64.2	21.4	121.8
11	Center	450	120	2	31.2	63.1	21.0	121.8
12	Factorial	300	60	1	41.1	43.6	14.54	94.5
13	Center	450	120	2	32.1	61.3	20.40	121.7
14	Axial	702	120	2	25.3	78.3	26.10	180.1
15	Center	450	120	2	31.3	63.4	21.1333	122.5
16	Center	450	120	2	31.2	63.5	21.1667	122.5
17	Axial	450	120	3.68	32.7	65.2	21.7333	124.5
18	Factorial	600	180	1	27.3	71.4	23.8	173.5
19	Factorial	300	180	3	31.3	45.6	15.2	103.5
20	Factorial	600	180	3	27.2	72.5	24.1667	168.4

Note: CCD is Central Composite Designs and SSA is Specific Surface Area.

3.7.2. Analysis of Variance (ANOVA)

The ANOVA findings revealed that the actual relationship between each of the responses and relevant variables was adequately expressed by equations (Supplementary Information). The ANOVA findings for the quadratic model for the Kenaf biochar yield, cadmium removal rate, adsorption capacity, and surface area showed model F-values of 23.83, 45.3, 30.08, and 34.78 and suggested that the three models were significant. The values of $\text{prob} > F$ of less than 0.05 indicated that the model terms were significant. In this case, temperature (X_1), heating time (X_3), and the interaction (X_{12}) were significant model terms, while the impregnation ratio (X_3) and the interaction terms (X_1X_3 , X_2X_3 , X_{22} , and X_{32}) were all insignificant to the biochar yield.

The plot between predicted versus experimental (real) data for the biochar yield and removal rate of cadmium, adsorption capacity, and specific surface area are shown in Figure 8a–d. The predicted values obtained were very similar to the experimental values, suggesting that the models developed were effective in representing the interaction connection between the biochar-based adsorbent preparation variables for the four responses. An analysis of the studentized residuals of responses confirmed that the selection model provides a proper approximation of the real system. The residuals followed a normal distribution (Supplementary Information).

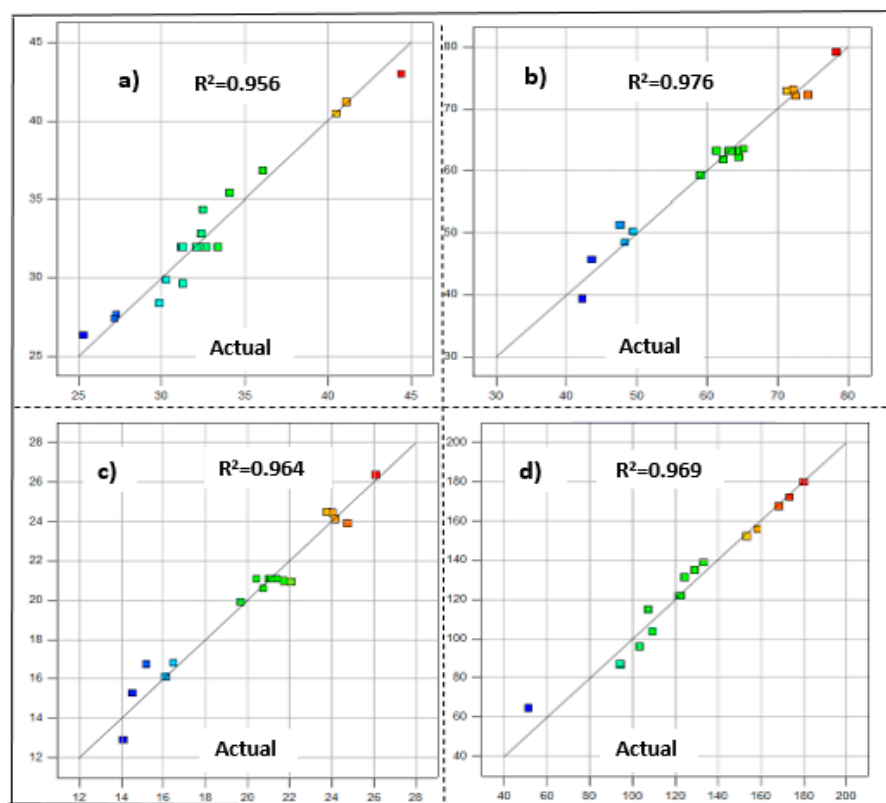


Figure 8. Correlation between the actual and predicted (software-based) values of (a) the Kenaf biochar yield, (b) cadmium removal rate, (c) adsorption capacity, and (d) specific surface areas of biochar.

3.8. The Combined Effect of Process Variables

The temperature was found to negatively affect the biochar yield but positively affect the quality of the biochar. The chemical and physical properties of biochar, including pore size distribution, defined the available pore volumes of carbon over three pore size regions: the micropore, mesopore, and macropore regions [73]. The inclusion of the characteristics of the impregnated biochar was not possible in this study and is seen worthy of a more detailed follow-up study.

The temperature was found to highly negatively affecting the biochar yield with the highest F-value of 179.49. Meanwhile, the heating time showed a slight effect on the biochar yield with the highest F-value of 21.51, whereas the chemical impregnation ratio showed a marginal effect on the response compared to temperature and time. The quadratic effect of temperature on the yield was also larger compared to the activation time and chemical impregnation ratio. However, the interaction effects between the variables were less significant.

Figure 9 shows the three-dimensional response surfaces showing the effects of the impregnated biochar preparation variables on the biochar yield (Y_1). It shows the relationship between temperature and reaction time. It can be seen that low temperatures and low times produce more char, which means that both parameters play an important role in the development of biochar.

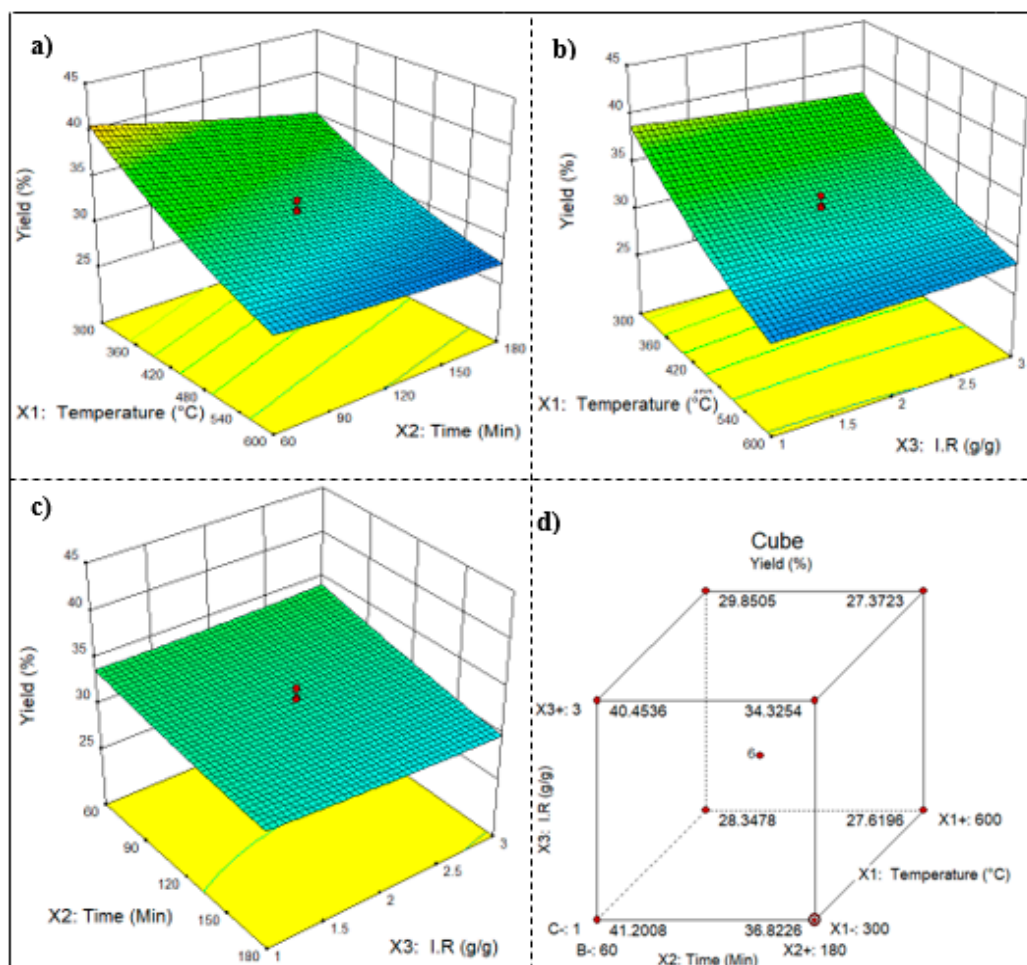


Figure 9. The combined effect of processing variables (a) temperature and time, (b) temperature and impregnation ratio, and (c) time and impregnation ratio on the biochar yield and (d) the biochar yield at each factorial point.

Figure 9b illustrates the interaction between temperature and the chemical impregnation ratio. The temperature affected the biochar qualitatively and quantitatively, while the chemical impregnation qualitatively affected the biochar. Since the biochar yield is considered qualitative, the interaction between temperature and chemical impregnation was small on the biochar yield compared to the interaction between temperature and reaction time [66]. By looking at the biochar yield at each factorial point in Figure 9d, biochar yields decreased with the increasing pyrolysis temperature, reaction time, and chemical impregnation ratio. The maximum yield was reached when all three variables were at the minimum points. This finding is also consistent with the work carried out by Siddiqui et al. [46], where temperature and time had major roles in the yield of biochar derived from pomegranate peel. The explanation for this decrease in biochar yield is that, as the temperature increased, volatile emissions occurred as a result of an increase in the dehydration and elimination reactions, as well as an increase in the C-NaOH and nitrogen reaction rates during pyrolysis [74].

The response surface three-dimensional diagrams and contour diagrams of the interaction of the pyrolysis temperature (X_1), reaction time (X_2), and impregnation ratio (X_3) on the removal rate of cadmium and adsorption capacity are presented in Figures 10 and 11, respectively. It can be seen from the curvature contour diagram that the response surface of temperature for the removal rate and adsorption capacity is greater than the time and impregnation ratio.

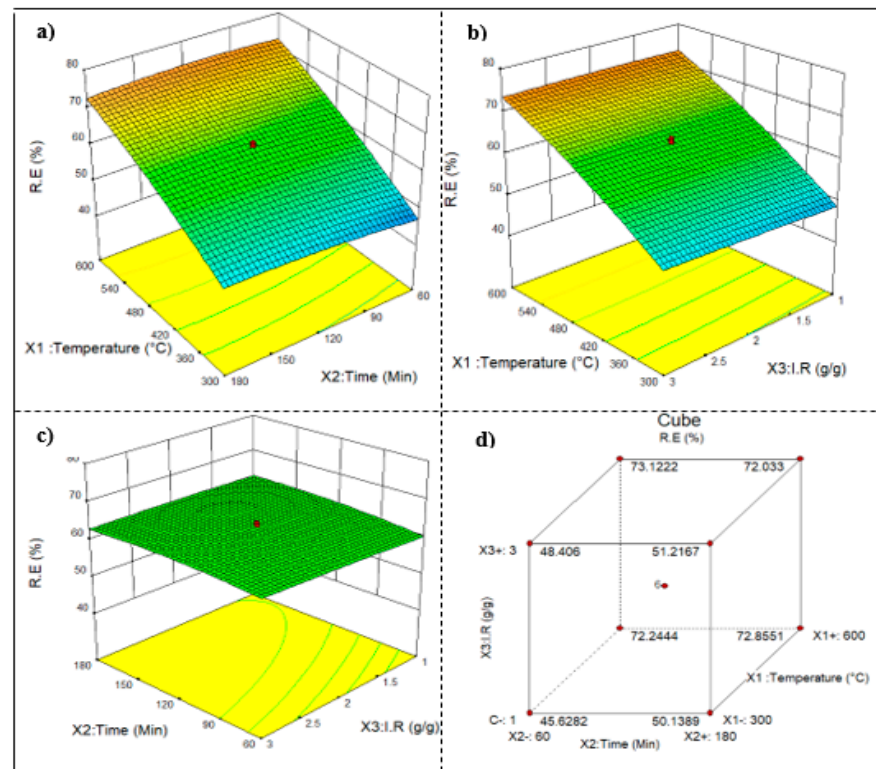


Figure 10. The combined effect of the process variables (a) temperature and time, (b) temperature and impregnation ratio, (c) time and impregnation ratio on cadmium (Cd) (II) removal, with the interaction effect of dual factors, and (d) removal percentage of cadmium at each factorial point.

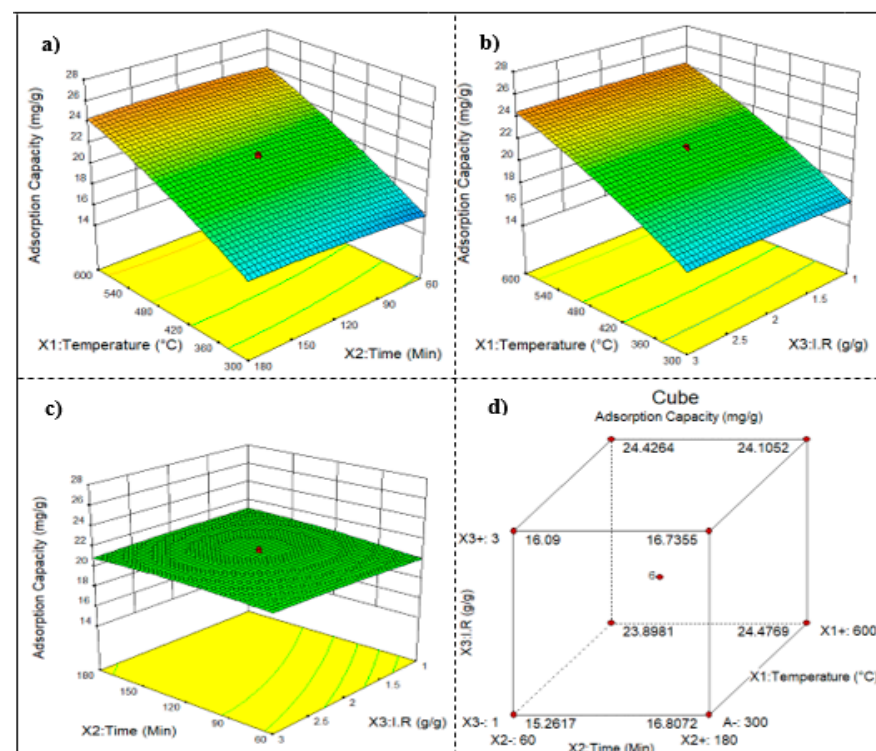


Figure 11. The combined effect of the process variables (a) temperature and time, (b) temperature and impregnation ratio, (c) time and impregnation ratio on the cadmium adsorption capacity, with the interaction effect of dual factors, and (d) cadmium adsorption capacity at each factorial point.

The response surface three-dimensional diagrams and contour diagrams of the interaction of pyrolysis temperature (X_1), reaction time (X_2), and impregnation ratio (X_3) on the specific surface area of the Kenaf biochar presented in Figure 12. The temperature positively affects the biochar surface area. The temperature was found to have the greatest positive effect on the specific surface area with the highest F-value of 294.54, while time shows a small effect on the biochar surface area with the F-value of 12.7. The chemical impregnation ratio shows a good effect on the specific surface area with the F-value of 13.15.

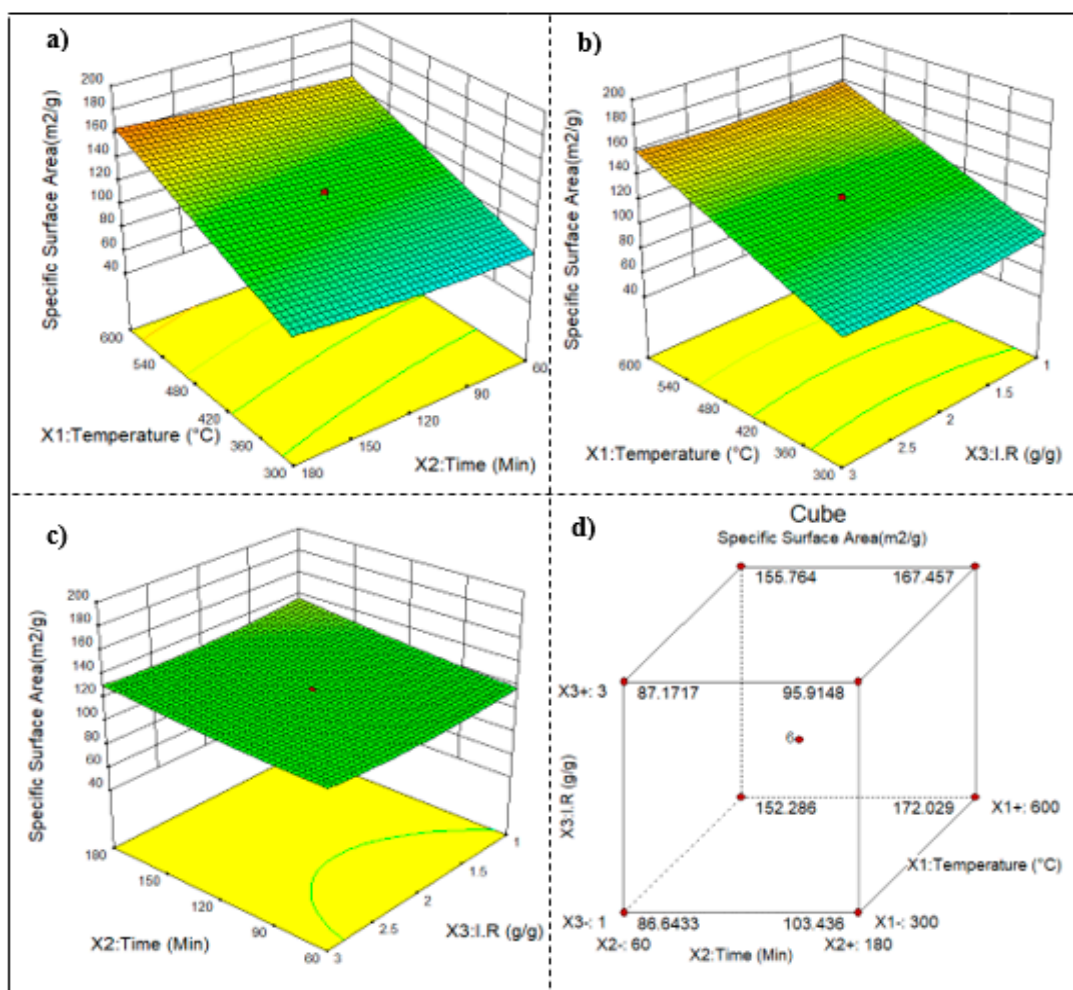


Figure 12. The combined effect of the process variables (a) temperature and time, (b) temperature and impregnation ratio, (c) time and impregnation ratio on the specific surface area of biochar, with the interaction effect of dual factors, and (d) the specific surface area of biochar at each factorial point.

3.9. Process Optimization

Due to the different areas of interest, it is very difficult to optimize all the responses that make the product more effective and economical. There are the two most important responses that industries are focusing on: yield and adsorption capacity [75]. Recently, researchers have focused more on the surface modification of products. Economic viability comes first, then specific modifications based on the targeting pollutants that they want to remove. From a sustainable perspective, it is necessary to recycle some of the wastes, such as agricultural waste (biomass from the second or third crops, residues of harvest, and waste collection) [76]. For this reason, when adsorbents are made from waste, researchers usually use surface modifications. From the above analysis, the product yield (Y_1) increases as the removal rate (Y_2), adsorption capacity (Y_3), and specific surface area (Y_4) decrease and vice versa. Therefore, to make a compromise between these responses, Design-Expert

software (DOE) was used to apply the desired functions. The experimental condition with the highest desirability (66.70%) was selected for verification. Biochar was prepared under the experimental conditions presented in Table 3, along with the experimental values for yield, removal rate, and adsorption capacity. It was noted that the experimental values obtained were in good agreement with the values determined from the models. The optimal Kenaf biochar was obtained using 550 °C temperature, 180 min of reaction time, and a 1:1 impregnation ratio, resulting in 28.6% of the biochar yield, 69.82% of the cadmium removal, 23.48 mg/g of the adsorption capacity, and 160.44 m²/g of biochar-specific area.

Table 3. Complementary Design–Expert software (DOE) validation of the quadratic mathematical model.

Temperature, x_1 (°C)	Time, x_2 (min)	NaOH Impregnation Ratio, x_3 (g/g)	Yield, Y_1 (%)	Cd ²⁺ Removal, Y_2 (%)	Adsorption Capacity, Y_3 (mg/g)	Biochar SSA Y_4 (m ² /g)	Desirability
550	180	1	28.60	69.82	23.48	160.44	0.667

4. Conclusions

The biochar-based adsorbent derived from Kenaf fiber was demonstrated to be a good adsorbent for the removal of cadmium from an aqueous solution. However, the impact of preparation parameters often offset each other, necessitating an optimization. With the help of a design expert, the regression analysis and variable optimizations were developed and showed a good fit with the experimental data. Based on the optimization results, the pyrolysis temperature was found as the most significant factor among all the processing variables. The optimal Kenaf biochar was obtained using 550 °C, 180 min of reaction time, and a 1:1 impregnation ratio. The resulting adsorbent had a 28.6% biochar yield, 69.82% cadmium removal, 23.48 mg/g adsorption capacity, and 160.44 m²/g biochar-specific surface area. The findings of this study demonstrate the effectiveness of the RSM for multiparametric optimization.

Supplementary Materials: The following are available online at <https://www.mdpi.com/article/10.3390/w13070999/s1>.

Author Contributions: Conceptualization, A.A.H.S., N.Y.H., and S.S.; methodology, A.A.H.S. and N.Y.H.; software, A.A.H.S. and A.A.S.G.; validation, A.A.H.S., M.R.B., and N.Y.H.; formal analysis, A.A.H.S. and Z.Y.Z.; investigation, A.A.H.S., A.H.J., and B.N.S.A.-D.; resources, A.A.H.S. and N.Y.H.; data curation, B.A.N. and N.M.I.; writing—original draft preparation, A.A.H.S. and M.R.B.; writing—review and editing, M.R.B. and A.H.J.; visualization, A.A.S.G. and B.N.S.A.-D.; supervision, A.A.H.S. and S.S.; project administration, A.A.H.S. and N.Y.H.; and funding acquisition, B.A.N. and N.M.I. All authors have read and agreed to the published version of the manuscript.

Funding: This work was funded by the Yayasan Universiti Teknologi PETRONAS (YUTP) with grant code YUTP-015LC0-210. The APC was funded by Universiti Malaysia Sabah.

Data Availability Statement: The data presented in this study are available from the corresponding author upon reasonable request.

Acknowledgments: The authors would like to acknowledge the efforts of the Universiti Teknologi Petronas Malaysia for financing the project through Yayasan Universiti Teknologi PETRONAS (YUTP) with grant code YUTP-015LC0-210.

Conflicts of Interest: The authors declare no conflict of interest.

References

1. Wang, G.; Li, A.; Li, M. Sorption of nickel ions from aqueous solutions using activated carbon derived from walnut shell waste. *Desalination Water Treat.* **2010**, *16*, 282–289. [[CrossRef](#)]
2. Saeed, A.; Harun, N.; Sufian, S.; Siyal, A.; Zulfiqar, M.; Bilad, M.; Vagananthan, A.; Al-Fakih, A.; Ghaleb, A.; Almahbashi, N. *Eucheuma cottonii* Seaweed-Based Biochar for Adsorption of Methylene Blue Dye. *Sustainability* **2020**, *12*, 10318. [[CrossRef](#)]
3. Sharma, S.K. *Heavy Metals in Water: Presence, Removal and Safety*; Royal Society of Chemistry: London, UK, 2014.

4. Isam, M.; Baloo, L.; Kutty, S.R.M.; Yavari, S. Optimisation and Modelling of Pb (II) and Cu (II) Biosorption onto Red Algae (*Gracilaria changii*) by Using Response Surface Methodology. *Water* **2019**, *11*, 2325. [[CrossRef](#)]
5. Arshad, H.; Mehmood, M.Z.; Shah, M.H.; Abbasi, A.M. Evaluation of heavy metals in cosmetic products and their health risk assessment. *Saudi Pharm. J.* **2020**, *28*, 779–790. [[CrossRef](#)] [[PubMed](#)]
6. Hezam Saeed, A.A.; Harun, N.Y.; Sufian, S.; Bin Aznan, M.F. Effect of Adsorption Parameter on the Removal of Nickel (II) by Low-Cost Adsorbent Extracted From Corn Cob. *Int. J. Adv. Res. Eng. Technol.* **2020**, *11*, 981–989.
7. Saeed, A.A.H.; Harun, N.Y.; Zulfani, N. Heavy Metals Capture from Water Sludge by Kenaf Fibre Activated Carbon in Batch Adsorption. *J. Ecol. Eng.* **2020**, *21*, 102–115. [[CrossRef](#)]
8. Kanawade, S.M.; Gaikwad, R. Adsorption of heavy metals by activated carbon synthesized from solid wastes. *Int. J. Chem. Eng. Appl.* **2011**, *2*, 207–211. [[CrossRef](#)]
9. Jagaba, A.; Kutty, S.; Hayder, G.; Baloo, L.; Abubakar, S.; Ghaleb, A.; Lawal, I.; Noor, A.; Umaru, I.; Almahbashi, N. Water quality hazard assessment for hand dug wells in Rafin Zurfi, Bauchi State, Nigeria. *Ain Shams Eng. J.* **2020**, *11*, 983–999. [[CrossRef](#)]
10. Naja, G.M.; Volesky, B. Toxicity and sources of Pb, Cd, Hg, Cr, As, and radionuclides in the environment. *Heavy Met. Environ.* **2009**, *8*, 16–18.
11. Simeng, L.; Chen, G. Using hydrogel-Biochar composites for enhanced cadmium removal from aqueous media. *Mater. Sci. Eng.* **2018**, *2*, 294–298.
12. Kim, J.-J.; Kim, Y.-S.; Kumar, V. Heavy metal toxicity: An update of chelating therapeutic strategies. *J. Trace Elem. Med. Biol.* **2019**, *54*, 226–231. [[CrossRef](#)]
13. Pyrzynska, K. Removal of cadmium from wastewaters with low-cost adsorbents. *J. Environ. Chem. Eng.* **2019**, *7*, 102795. [[CrossRef](#)]
14. Khan, T.; Isa, M.; Mustafa, M. Artificial neural network approach for modeling of Cd (II) adsorption from aqueous solution by incinerated rice husk carbon. In Proceedings of the 3rd International Conference on Civil, Offshore and Environmental Engineering, Kuala Lumpur, Malaysia, 15–17 August 2016.
15. Flick, D.; Kraybill, H.; Dmitroff, J. Toxic effects of cadmium: A review. *Environ. Res.* **1971**, *4*, 71–85. [[CrossRef](#)]
16. World Health Organization. *Cadmium: Environmental Aspects*; World Health Organization: Geneva, Switzerland, 1992.
17. Bogusz, A.; Oleszczuk, P. Effect of biochar addition to sewage sludge on cadmium, copper and lead speciation in sewage sludge-amended soil. *Chemosphere* **2020**, *239*, 124719. [[CrossRef](#)]
18. Jagaba, A.; Kutty, S.; Hayder, G.; Baloo, L.; Ghaleb, A.; Lawal, I.; Abubakar, S.; Al-Dhawi, B.; Almahbashi, N.; Umaru, I. Degradation of Cd, Cu, Fe, Mn, Pb and Zn by *Moringa-oleifera*, zeolite, ferric-chloride, chitosan and alum in an industrial effluent. *Ain Shams Eng. J.* **2021**, *12*, 57–64. [[CrossRef](#)]
19. Agarwal, R.M.; Singh, K. Methodologies for removal of heavy metal ions from wastewater: An overview. *Interdiscip. Environ. Rev.* **2017**, *18*, 124–142.
20. Jagaba, A.H.; Abubakar, S.; Nasara, M.A.; Jagaba, S.M.; Chamah, H.M.; Lawal, I.M. Defluoridation of Drinking Water by Activated Carbon Prepared from *Tridax Procumbens* Plant (Gashaka Village, Hong L. G. A., Adamawa State, Nigeria). *Int. J. Comput. Theor. Chem.* **2019**, *7*, 1–5. [[CrossRef](#)]
21. Khan, T.; Ab Wahap, S.A.B.; Chaudhuri, M. Adsorption of arsenite from water by rice husk silica. *Nat. Environ. Pollut. Technol.* **2012**, *11*, 229–233.
22. Lei, Y.; Chen, F.; Luo, Y.; Zhang, L. Synthesis of three-dimensional graphene oxide foam for the removal of heavy metal ions. *Chem. Phys. Lett.* **2014**, *593*, 122–127. [[CrossRef](#)]
23. Li, D.; Tian, X.; Wang, Z.; Guan, Z.; Li, X.; Qiao, H.; Ke, H.; Luo, L.; Wei, Q. Multifunctional adsorbent based on metal-organic framework modified bacterial cellulose/chitosan composite aerogel for high efficient removal of heavy metal ion and organic pollutant. *Chem. Eng. J.* **2020**, *383*, 123127. [[CrossRef](#)]
24. He, K.; Chen, Y.; Tang, Z.; Hu, Y. Removal of heavy metal ions from aqueous solution by zeolite synthesized from fly ash. *Environ. Sci. Pollut. Res.* **2015**, *23*, 2778–2788. [[CrossRef](#)] [[PubMed](#)]
25. Lee, H.W.; Kim, Y.M.; Kim, S.; Ryu, C.; Park, S.H.; Park, Y.K. Review of the use of activated biochar for energy and environmental applications. *Carbon Lett.* **2018**, *26*, 1–10.
26. Fiyadh, S.S.; AlSaadi, M.A.; Jaafar, W.Z.; AlOmar, M.K.; Fayaed, S.S.; Mohd, N.S.; Hin, L.S.; El-Shafie, A. Review on heavy metal adsorption processes by carbon nanotubes. *J. Clean. Prod.* **2019**, *230*, 783–793. [[CrossRef](#)]
27. Ani, J.U.; Akpomie, K.G.; Okoro, U.C.; Aneke, L.E.; Onukwuli, O.D.; Ujam, O.T. Potentials of activated carbon produced from biomass materials for sequestration of dyes, heavy metals, and crude oil components from aqueous environment. *Appl. Water Sci.* **2020**, *10*, 69. [[CrossRef](#)]
28. Komkiene, J.; Baltreinaite, E. Baltreinaite, and Technology, Biochar as adsorbent for removal of heavy metal ions [Cadmium (II), Copper (II), Lead (II), Zinc (II)] from aqueous phase. *Environ. Sci. Technol.* **2016**, *13*, 471–482.
29. Saeed, A.A.H.; Harun, N.Y.; Sufian, S.; Afolabi, H.K.; Al-Qadami, E.H.H.; Roslan, F.A.S.; Rahim, S.A.; Ghaleb, A.S. Production and Characterization of Rice Husk Biochar and Kenaf Biochar for Value-Added Biochar Replacement for Potential Materials Adsorption. *Ecol. Eng. Environ. Technol.* **2021**, *22*, 1–8. [[CrossRef](#)]
30. Millogo, Y.; Aubert, J.-E.; Hamard, E.; Morel, J.-C. How Properties of Kenaf Fibers from Burkina Faso Contribute to the Reinforcement of Earth Blocks. *Materials* **2015**, *8*, 2332–2345. [[CrossRef](#)]
31. Noor, N.M.; Othman, R.; Mubarak, N.; Abdullah, E.C. Agricultural biomass-derived magnetic adsorbents: Preparation and application for heavy metals removal. *J. Taiwan Inst. Chem. Eng.* **2017**, *78*, 168–177. [[CrossRef](#)]

32. Saeed, A.; Harun, N.Y.; Bilad, M.; Afzal, M.; Parvez, A.; Roslan, F.; Rahim, S.A.; Vinayagam, V.; Afolabi, H. Moisture Content Impact on Properties of Briquette Produced from Rice Husk Waste. *Sustainability* **2021**, *13*, 3069. [[CrossRef](#)]
33. Saeed, A.A.H.; Harun, N.Y.; Nasef, M.M. Physicochemical characterization of different agricultural residues in malaysia for bio char production. *Int. J. Civ. Eng. Technol.* **2019**, *10*, 213–225.
34. Jagaba, A.; Kutty, S.; Lawal, I.; Abubakar, S.; Hassan, I.; Zubairu, I.; Umaru, I.; Abdurrasheed, A.; Adam, A.; Ghaleb, A.; et al. Sequencing batch reactor technology for landfill leachate treatment: A state-of-the-art review. *J. Environ. Manag.* **2021**, *282*, 111946. [[CrossRef](#)]
35. Zhang, H.; Yue, X.; Li, F.; Xiao, R.; Zhang, Y.; Gu, D. Preparation of rice straw-derived biochar for efficient cadmium removal by modification of oxygen-containing functional groups. *Sci. Total Environ.* **2018**, *631*, 795–802. [[CrossRef](#)]
36. Gupta, S.; Sireesha, S.; Sreedhar, I.; Patel, C.M.; Anitha, K. Latest trends in heavy metal removal from wastewater by biochar based sorbents. *J. Water Process. Eng.* **2020**, *38*, 101561. [[CrossRef](#)]
37. Ghaleb, A.A.S.; Kutty, S.R.M.; Ho, Y.-C.; Jagaba, A.H.; Noor, A.; Al-Sabaei, A.M.; Almahbashi, N.M.Y. Response Surface Methodology to Optimize Methane Production from Mesophilic Anaerobic Co-Digestion of Oily-Biological Sludge and Sugarcane Bagasse. *Sustainability* **2020**, *12*, 2116. [[CrossRef](#)]
38. Lye, H.L.; Mohammed, B.S.; Liew, M.; Wahab, M.; Al-Fakih, A. Bond behaviour of CFRP-strengthened ECC using Response Surface Methodology (RSM). *Case Stud. Constr. Mater.* **2020**, *12*, e00327. [[CrossRef](#)]
39. Karacan, F.; Ozden, U.; Karacan, S. Optimization of manufacturing conditions for activated carbon from Turkish lignite by chemical activation using response surface methodology. *Appl. Therm. Eng.* **2007**, *27*, 1212–1218. [[CrossRef](#)]
40. Baçaoui, A.; Yaacoubi, A.; Dahbi, A.; Bennouna, C.; Luu, R.P.T.; Maldonado-Hodar, F.; Rivera-Utrilla, J.; Moreno-Castilla, C. Optimization of conditions for the preparation of activated carbons from olive-waste cakes. *Carbon* **2001**, *39*, 425–432. [[CrossRef](#)]
41. Saeed, A.A.H.; Harun, N.Y.; Nasef, M.M.; Afolabi, H.K.; Ghaleb, A.A.S. Removal of Cadmium from Aqueous Solution by Optimized Magnetic Biochar Using Response Surface Methodology. In Proceedings of the International Conference on Civil, Offshore and Environmental Engineering, Kuching, Malaysia, 13–15 July 2021; Metzler, J.B., Ed.; Springer: Singapore; pp. 119–126.
42. Azargohar, R.; Dalai, A. Production of activated carbon from Luscar char: Experimental and modeling studies. *Microporous Mesoporous Mater.* **2005**, *85*, 219–225. [[CrossRef](#)]
43. Kasman, M.; Ibrahim, S. Application of response surface methodology in optimization of cadmium adsorption by raw rice husk. In Proceedings of the 2010 International Conference on Chemistry and Chemical Engineering, Kyoto, Japan, 1–3 August 2010.
44. Khan, T.; Mustafa, M.R.U.; Isa, M.H.; Manan, T.S.B.A.; Ho, Y.-C.; Lim, J.-W.; Yusof, N.Z. Artificial Neural Network (ANN) for Modelling Adsorption of Lead (Pb (II)) from Aqueous Solution. *Water Air Soil Pollut.* **2017**, *228*, 426. [[CrossRef](#)]
45. Iwar, R.T.; Ogedengbe, K.; Okwuchukwu, P. Column Studies on the Adsorption of Cadmium (Cd) in Aqueous Solution on Raffia Palm Seed (*Raphia Hookeri*) Activated Carbon. *Am. J. Environ. Eng. Sci.* **2018**, *5*, 38–45.
46. Siddiqui, M.T.H.; Nizamuddin, S.; Mubarak, N.M.; Shirin, K.; Aijaz, M.; Hussain, M.; Baloch, H.A. Characterization and Process Optimization of Biochar Produced Using Novel Biomass, Waste Pomegranate Peel: A Response Surface Methodology Approach. *Waste Biomass Valorization* **2019**, *10*, 521–532. [[CrossRef](#)]
47. Tee, Y.B.; Talib, R.A.; Abdan, K.; Chin, N.L.; Basha, R.K.; Yunos, K.F.M. Thermally Grafting Aminosilane onto Kenaf-Derived Cellulose and Its Influence on the Thermal Properties of Poly(Lactic Acid) Composites. *BioResources* **2013**, *8*, 4468–4483. [[CrossRef](#)]
48. Kawamoto, H. Lignin pyrolysis reactions. *J. Wood Sci.* **2017**, *63*, 117–132. [[CrossRef](#)]
49. Leng, L.; Huang, H. An overview of the effect of pyrolysis process parameters on biochar stability. *Bioresour. Technol.* **2018**, *270*, 627–642. [[CrossRef](#)]
50. Tripathi, M.; Sahu, J.; Ganesan, P. Effect of process parameters on production of biochar from biomass waste through pyrolysis: A review. *Renew. Sustain. Energy Rev.* **2016**, *55*, 467–481. [[CrossRef](#)]
51. Crombie, K.; Mašek, O.; Cross, A.; Sohi, S. Biochar-Synergies and trade-offs between soil enhancing properties and C sequestration potential. *GCB Bioenergy* **2014**, *7*, 1161–1175. [[CrossRef](#)]
52. Pereira, R.C.; Kaal, J.; Arbestain, M.C.; Lorenzo, R.P.; Aitkenhead, W.; Hedley, M.; Macías, F.; Hindmarsh, J.; Maciá-Agulló, J. Contribution to characterisation of biochar to estimate the labile fraction of carbon. *Org. Geochem.* **2011**, *42*, 1331–1342. [[CrossRef](#)]
53. Marrakchi, F.; Ahmed, M.; Khanday, W.; Asif, M.; Hameed, B. Mesoporous-activated carbon prepared from chitosan flakes via single-step sodium hydroxide activation for the adsorption of methylene blue. *Int. J. Biol. Macromol.* **2017**, *98*, 233–239. [[CrossRef](#)]
54. Tay, J.; Chen, X.; Jeyaseelan, S.; Graham, N. Optimising the preparation of activated carbon from digested sewage sludge and coconut husk. *Chemosphere* **2001**, *44*, 45–51. [[CrossRef](#)]
55. Givianrad, M.; Rabani, M.; Saber-Tehrani, M.; Aberoomand-Azar, P.; Sabzevari, M.H. Preparation and characterization of nanocomposite, silica aerogel, activated carbon and its adsorption properties for Cd (II) ions from aqueous solution. *J. Saudi Chem. Soc.* **2013**, *17*, 329–335. [[CrossRef](#)]
56. Hu, S.; Zhou, Y.; Zhou, L.; Huang, Y.; Zeng, Q. Study on the adsorption behavior of cadmium, copper, and lead ions on the crosslinked polyethylenimine dithiocarbamate material. *Environ. Sci. Pollut. Res.* **2018**, *27*, 2444–2454. [[CrossRef](#)]
57. Nizamuddin, S.; Shrestha, S.; Athar, S.; Ali, B.S.; Siddiqui, M.A. A critical analysis on palm kernel shell from oil palm industry as a feedstock for solid char production. *Rev. Chem. Eng.* **2016**, *32*, 489–505. [[CrossRef](#)]
58. Mašek, O.; Brownsort, P.; Cross, A.; Sohi, S. Influence of production conditions on the yield and environmental stability of biochar. *Fuel* **2013**, *103*, 151–155. [[CrossRef](#)]

59. Angin, D. Effect of pyrolysis temperature and heating rate on biochar obtained from pyrolysis of safflower seed press cake. *Bioresour. Technol.* **2013**, *128*, 593–597. [[CrossRef](#)]
60. Ben Hassen-Trabelsi, A.; Kraiem, T.; Naoui, S.; Belayouni, H. Pyrolysis of waste animal fats in a fixed-bed reactor: Production and characterization of bio-oil and bio-char. *Waste Manag.* **2014**, *34*, 210–218. [[CrossRef](#)]
61. Klasson, K.T. Biochar characterization and a method for estimating biochar quality from proximate analysis results. *Biomass Bioenergy* **2017**, *96*, 50–58. [[CrossRef](#)]
62. Spokas, K. Review of the stability of biochar in soils: Predictability of O: C molar ratios. *Carbon Manag.* **2010**, *1*, 289–303. [[CrossRef](#)]
63. Tangjuank, S.; Insuk, N.; Tontrakoon, J.; Udeye, V. Adsorption of lead (II) and cadmium (II) ions from aqueous solutions by adsorption on activated carbon prepared from cashew nut shells. *World Acad. Sci. Eng. Technol.* **2009**, *52*, 110–116.
64. Zhou, R.; Zhang, M.; Zhou, J.; Wang, J. Optimization of biochar preparation from the stem of *Eichhornia crassipes* using response surface methodology on adsorption of Cd²⁺. *Sci. Rep.* **2019**, *9*, 17538. [[CrossRef](#)]
65. Liatsou, I.; Michail, G.; Demetriou, M.; Pashalidis, I. Uranium binding by biochar fibres derived from *Luffa cylindrica* after controlled surface oxidation. *J. Radioanal. Nucl. Chem.* **2017**, *311*, 871–875. [[CrossRef](#)]
66. Mopoung, R.; Kengkhetkit, N. Lead and cadmium removal efficiency from aqueous solution by NaOH treated pineapple waste. *Int. J. Appl. Chem.* **2016**, *12*, 23–35.
67. Huang, P.-H.; Jhan, J.-W.; Cheng, Y.-M.; Cheng, H.-H. Effects of Carbonization Parameters of Moso-Bamboo-Based Porous Charcoal on Capturing Carbon Dioxide. *Sci. World J.* **2014**, *2014*, 937867. [[CrossRef](#)] [[PubMed](#)]
68. Yang, J.; Qiu, K. Development of high surface area mesoporous activated carbons from herb residues. *Chem. Eng. J.* **2011**, *167*, 148–154. [[CrossRef](#)]
69. Kumar, A.; Jena, H. Preparation and characterization of high surface area activated carbon from Fox nut (*Euryale ferox*) shell by chemical activation with H₃PO₄. *Results Phys.* **2016**, *6*, 651–658. [[CrossRef](#)]
70. Yang, J.; Qiu, K. Preparation of activated carbons from walnut shells via vacuum chemical activation and their application for methylene blue removal. *Chem. Eng. J.* **2010**, *165*, 209–217. [[CrossRef](#)]
71. Gao, X.; Wu, L.; Li, Z.; Xu, Q.; Tian, W.; Wang, R. Preparation and characterization of high surface area activated carbon from pine wood sawdust by fast activation with H₃PO₄ in a spouted bed. *J. Mater. Cycles Waste Manag.* **2017**, *20*, 925–936. [[CrossRef](#)]
72. Witek-Krowiak, A.; Chojnacka, K.; Podstawczyk, D.; Dawiec, A.; Pokomeda, K. Application of response surface methodology and artificial neural network methods in modelling and optimization of biosorption process. *Bioresour. Technol.* **2014**, *160*, 150–160. [[CrossRef](#)]
73. Shakoor, M.B.; Ali, S.; Rizwan, M.; Abbas, F.; Bibi, I.; Riaz, M.; Khalil, U.; Niazi, N.K.; Rinklebe, J. A review of biochar-based sorbents for separation of heavy metals from water. *Int. J. Phytoremediat.* **2020**, *22*, 111–126. [[CrossRef](#)]
74. Hassan, A.F.; Youssef, A.M. Preparation and characterization of microporous NaOH-activated carbons from hydrofluoric acid leached rice husk and its application for lead (II) adsorption. *Carbon Lett.* **2014**, *15*, 57–66. [[CrossRef](#)]
75. Saikia, R.; Goswami, R.; Bordoloi, N.; Senapati, K.K.; Pant, K.K.; Kumar, M.; Katak, R. Removal of arsenic and fluoride from aqueous solution by biomass based activated biochar: Optimization through response surface methodology. *J. Environ. Chem. Eng.* **2017**, *5*, 5528–5539. [[CrossRef](#)]
76. Sulaiman, N.S.; Hashim, R.; Amini, M.H.M.; Danish, M.; Sulaiman, O. Optimization of activated carbon preparation from cassava stem using response surface methodology on surface area and yield. *J. Clean. Prod.* **2018**, *198*, 1422–1430. [[CrossRef](#)]